*American Mineralogist, Volume 70, pages 1253–1261, 1985*

# Microstructures and orientation relationships in the dry-state aragonite–calcite and calcite–lime phase transformations

JOHN W. MCTIGUE, JR.[1] AND HANS-RUDOLF WENK

*Department of Geology and Geophysics*
*University of California, Berkeley, California 94720*

**Abstract**

The aragonite–calcite and calcite–lime transformations are observed in situ in the high voltage transmission electron microscope. Above 400°C aragonite single crystals begin to transform into calcite through heterogeneous nucleation on dislocations, twin boundaries, and modulated microstructures. Subsequent growth is generally topotactic with $(100)_A = (11\bar{2}0)_C$, $(010)_A \sim (\bar{1}104)_C$, $(011)_A \sim (0001)_C$, and $[001]_A \sim [r_2 : f_1]_C$ in the aragonite–calcite transition. Above 500°C calcite decomposes into lime and $CO_2$. This reaction is also topotactic with $(001)_L \sim (\bar{1}104)_C$, and $(\bar{1}\bar{1}1)_L \sim (0001)_C$. Movement of partial dislocations and propagation of stacking faults are not observed during the transformations. In situ observations therefore support a heterogeneous nucleation and interface-controlled growth mechanism rather than a martensitic mechanism for the aragonite–calcite transformation under the conditions of the experiment. Decomposition may proceed initially by loss of $CO_2$ from a relatively rigid framework.

## Introduction

The aragonite–calcite polymorphic phase transformation and the decomposition reaction, calcite to lime plus $CO_2$, have been extensively studied and widely debated (see below). Although X-ray diffraction and optical microscopy provide information on the topotaxy and bulk kinetics of the transformations, details of the mechanisms have not been resolved. In situ heating experiments in the high voltage transmission electron microscope, however, yield information on both the orientation relationships and the microstructures involved as the transformations proceed.

Aragonite, the high-pressure polymorph of $CaCO_3$ is metastable at low temperatures and atmospheric pressure. It transforms into calcite upon heating above 400°C. At higher temperatures and prolonged heating time calcite decomposes into lime (CaO) plus $CO_2$. The three mineral structures have similarities when viewed along [0001] and $[\bar{1}2\bar{1}0]$ in calcite, [001] and [100] in aragonite, and [111] and $[\bar{1}01]$ in lime respectively (Fig. 1). Lime is cubic and has the NaCl structure, and calcite is the rhombohedral derivative of it with $CO_3$ groups substituting for oxygen. Aragonite corresponds to the hexagonal close-packed analog. Crystallographic orientation relationships between calcite and aragonite have been documented by several studies (e.g., Brown et al., 1962; Dasgupta, 1964).

The correspondence between crystallographic planes and directions in the transformation suggests that an oriented martensitic mechanism is possible, as in fcc–hcp transformations in metal alloys (e.g., Barrett and Massalski, 1980, p. 486–495). Gillet and Madon (1982) proposed a martensitic mechanism involving the movement of partial dislocations in the basal plane, dragging stacking faults between them (with additional atomic shuffles) and producing the requisite change in stacking between aragonite and calcite structures. Carlson and Rosenfeld (1981) and Carlson (1982, 1983) argue that heterogeneous nucleation and interface-controlled growth on preferred planes and directions is a more likely mechanism. Both proposals suffer from an inability to resolve the transformation in progress at the scale of the appropriate microstructures.

Burrage and Pitkethly (1969) have performed an in situ experiment using beam-heating in a 100 keV transmission electron microscope, but the technique employed is qualitative, since temperatures can not be accurately recorded, and radiation damage during beam heating can destroy the specimen. High voltages (1500 keV) reduce the effects of ionization damage, and with a heating stage the temperature at the surface of the sample can be accurately measured. The high voltage transmission electron microscope (HVEM), equipped with a heating stage, provides a dynamic, high resolution laboratory for in situ analysis of changing diffraction conditions and contrast effects of microstructures involved in the aragonite–calcite and calcite–lime transformations.

## Materials and methods

Aragonite single crystals from Eugui, Spain, occurring in hydrothermal veins, have been cut normal to [001] and [100]. Thin sections are ion-thinned, carbon coated, and placed in a folding nickel grid, which immobilizes the specimen with a locking hinge. Grids are placed in a Swann side-entry, double-tilt heating stage. Analysis is performed in the Kratos 1500 keV instrument at the

[1] Present Address: Shell Development Co., P.O. Box 481, Houston, Texas, 77001.

0003–004X/85/1112–1253$02.00

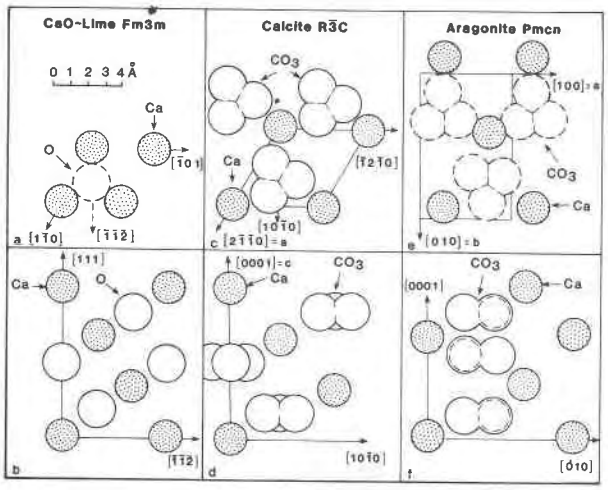


Fig. 1. Structural projections. (a) Lime (CaO) in a ⟨111⟩ orientation. Dotted circles: $Ca^{+}$. Open circles: $O^{2-}$. (b) Calcite in a ⟨0001⟩ orientation. (c) Aragonite in a ⟨001⟩ orientation. (d) Lime in a ⟨$\bar{1}$01⟩ orientation. (e) Calcite in a ⟨$\bar{1}2\bar{1}0$⟩ orientation. (f) Aragonite in a ⟨100⟩ orientation.

National Center for Electron Microscopy at the Lawrence Berkeley Laboratory.

In selected area diffraction (SAD) mode symmetrical orientations are obtained using the double-tilt stage. Heating proceeds with each orientation until calcite reflections begin to appear in the SAD pattern (Fig. 3). Orientation relationships are determined by indexing the aragonite and corresponding calcite patterns, which are then plotted in stereographic projection. Contrast changes in the bright-field and darkfield images are photographed to determine the extent of the transformation and the role of microstructures.

Temperatures in the heating stage are calibrated by heating quartz crystals to observe the high–low quartz transformation. Transformation occurs within 10°C of the well-documented 573°C as documented by the appearance of Dauphine twins during cooling (Van Tendeloo et al., 1975).

## Results

When the temperature is slowly raised to 400°C, there is little noticeable effect on the sample. Above 400°C the thin foil begins to shift and buckle (Fig. 2), requiring minor adjustments in tilt to maintain a desired orientation. The aragonite–calcite transformation involves a 7–10% in-

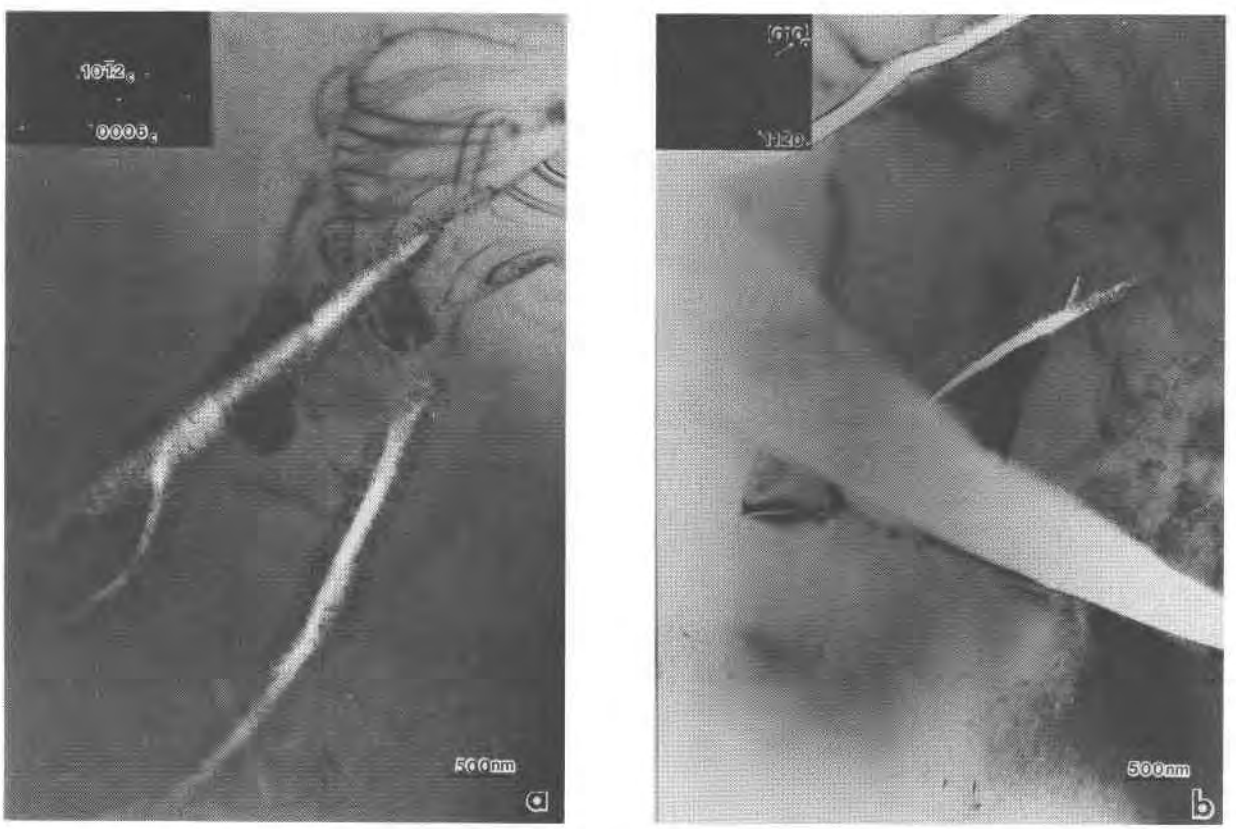


Fig. 2. (a) Incipient microfractures in aragonite due to rapid heating and transformation to calcite. (b) Microfractures separate as the thin foil shifts and buckles.

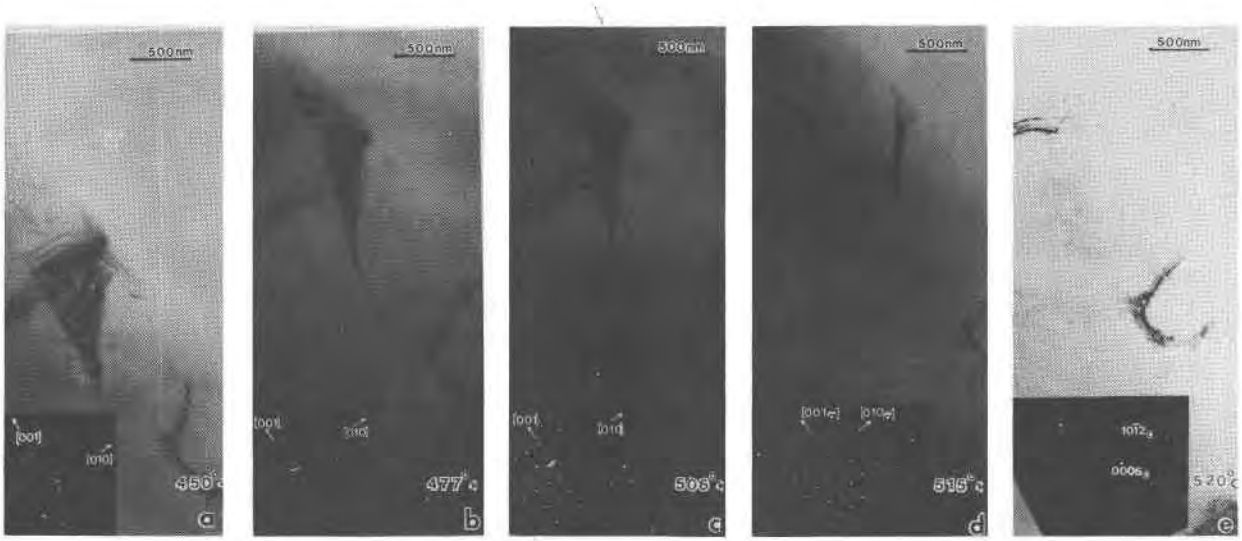


Fig. 3. (a–d) Aragonite grain (dark) transforms to calcite as grain boundary migrates across the thin foil, SAD inset. (e) Aragonite is completely consumed by calcite.

crease in volume, which accounts for the observed shifting and buckling. The aragonite single crystal may fracture before transformation is complete (Fig. 2). By raising the temperature slowly (less than 5°C per minute) and allowing the sample to equilibrate at each step, motion and misorientation are minimized.

Transformation at macroscopic rates (in the order of minutes) requires heating above 500°C. The appearance of

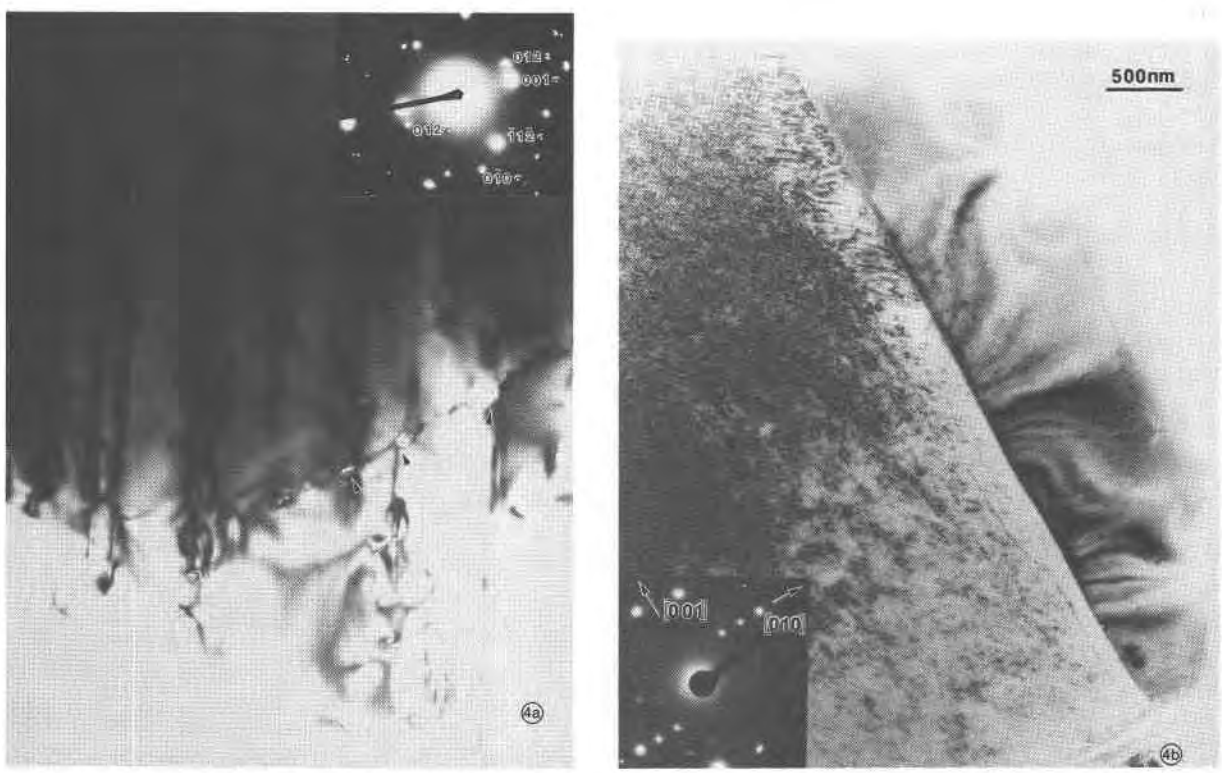


Fig. 4. (a) Calcite nucleii at the intersection of {110} twins and a dislocation in aragonite (arrowed). Dual phase diffraction pattern is inset. (b) Aragonite (right)–calcite (left) grain boundary oriented parallel to (010) in aragonite. Mottled contrast in calcite is due to radiation damage. Note microfracture in the lower right corner.

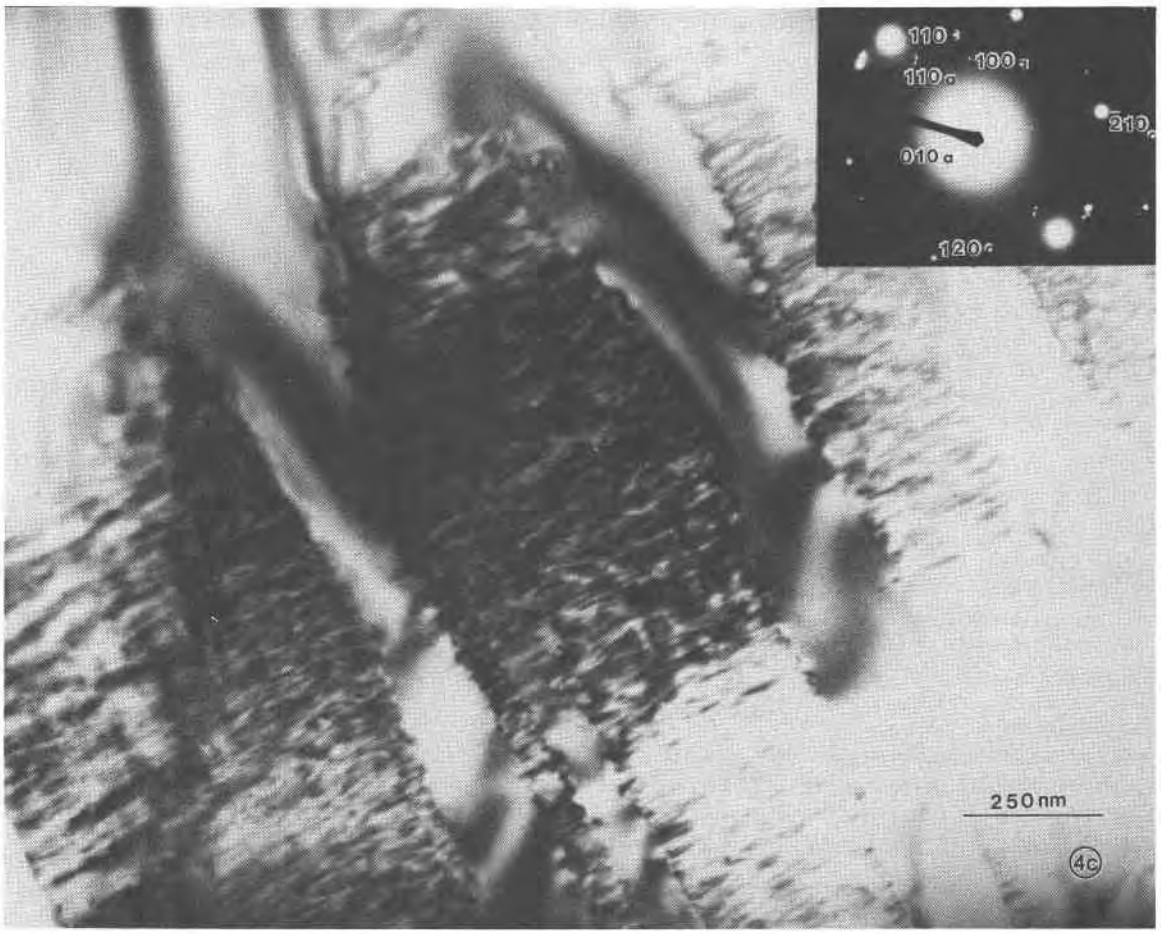


Fig. 4c. Modulated microstructure in lamellar domains of aragonite. Homogeneous interlamellar material is calcite.

noncommensurate reflections in the aragonite SAD pattern signals the onset of transformation to calcite.

Brightfield images reveal microstructural controls on the aragonite-calcite transformation. Calcite nucleates preferentially at the thin edge of the sample (Fig. 3a) and at defects, such as the intersection of a twin boundary and a dislocation (Fig. 4a). Growth proceeds through movement of oriented grain boundaries, which sweep across the thin foil until aragonite is consumed by calcite (Fig. 3a–d). The transformation interface maintains its sharp, linear appearance during migration (Fig. 4b).

A modulated microstructure appears in some lamellar domains of the aragonite (Fig. 4c). Although the structural nature of the modulations has not been determined, upon heating they slowly homogenize and disappear. An irregular boundary migrates through the modulated structure with calcite precipitating behind the boundary (Fig. 5a–c). White spots superimposed on both aragonite and calcite appear to be centers of incipient radiation damage and possible amorphization (Fig. 5b, c). Disintegration of the modulated microstructure is most rapid in relatively homogeneous regions between lamellar twins and individual septa of the modulated structure (Fig. 4d). Calcite precipi-

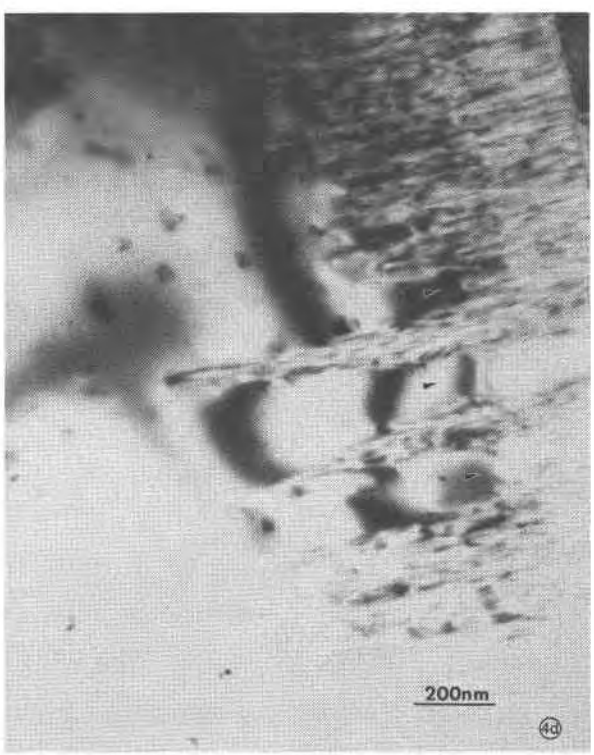


Fig. 4d. Transformation to calcite between individual septa (arrows) of the modulated structure in aragonite.

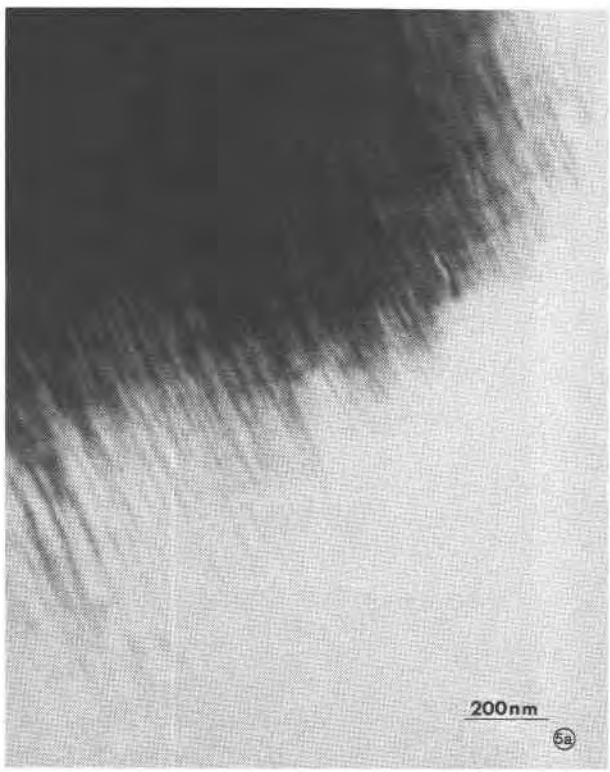


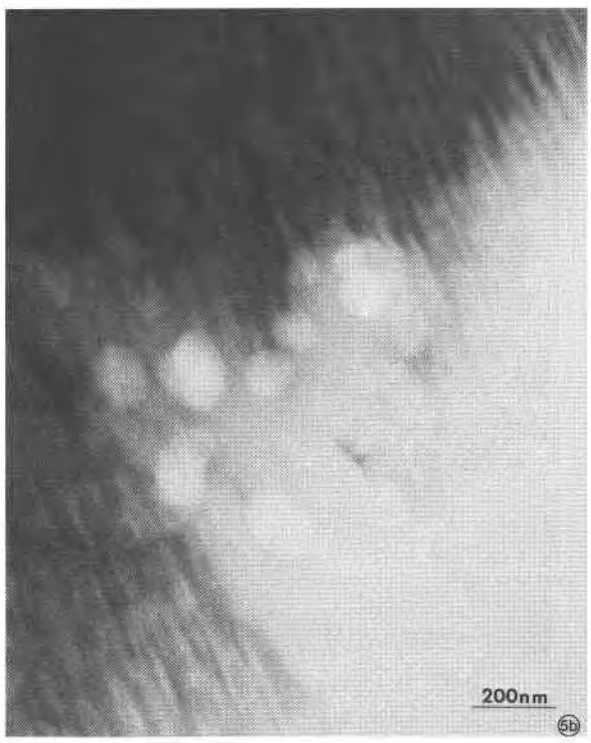


Fig. 5. (a–c) Irregular transformation (homogenization) boundary migrates through the modulated microstructure in aragonite. Calcite precipitates behind the boundary. White spots appear to be incipient radiation damage or amorphization.

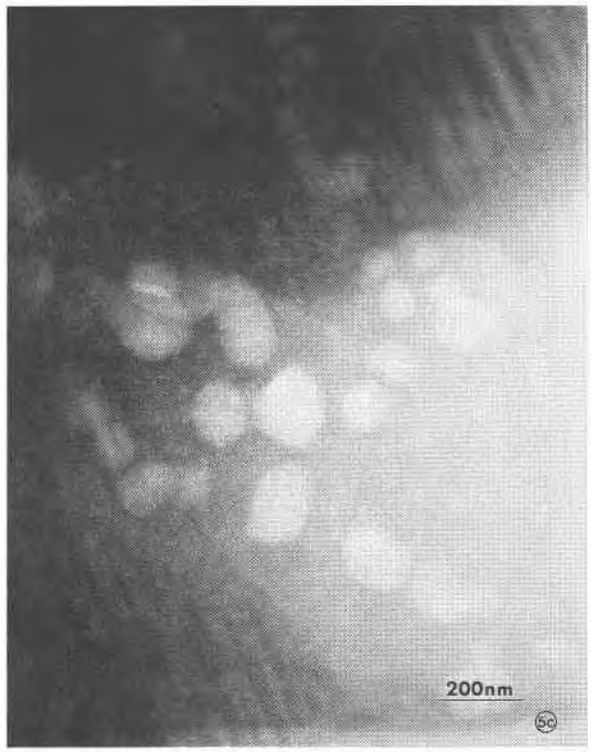


tating behind the homogenization boundary is relatively defect-free. At no time are partial dislocations or stacking faults observed propagating at the transformation interface.

Orientation relations are best documented in diffraction patterns. An aragonite $\langle 100 \rangle$ SAD (Fig. 6a) transforms into a calcite $\langle 11\bar{2}0 \rangle$ SAD (Fig. 6b). The stereographic projection illustrates the coincidences of planes and directions between aragonite and calcite (Fig. 6c). In this case, $(100)_A = (11\bar{2}0)_C$, $(010)_A \sim (\bar{1}104)_C$, $(011)_A = (0001)_C$, and $[001]_A \sim [r_2 : f_1]_C$. These observations correct a previously reported orientation relation in which $(001)_A \sim (\bar{1}012)_C$ (Wenk and McTigue, 1983).

Rings in the SAD pattern indicate contemporaneous development of polycrystalline lime through decomposition of calcite above 500°C (Fig. 7). Heterogeneous density of intensity in the lime rings suggest preferred orientation of lime crystallites with respect to the calcite precursor. If centers of heterogeneous intensity in the rings are indexed as if they formed a single crystal pattern, an orientation

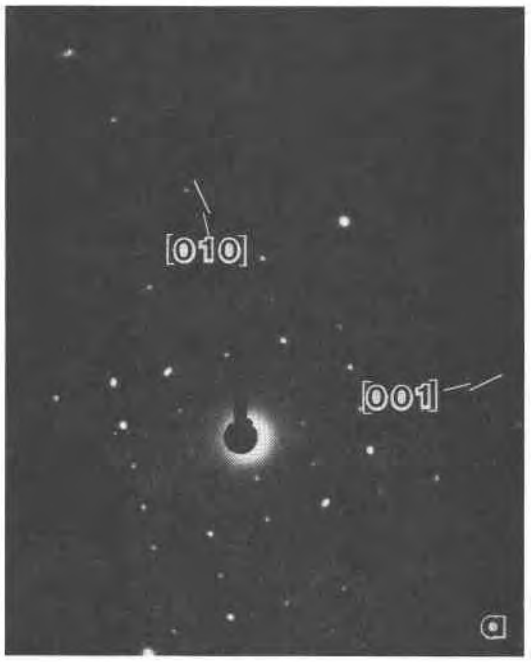


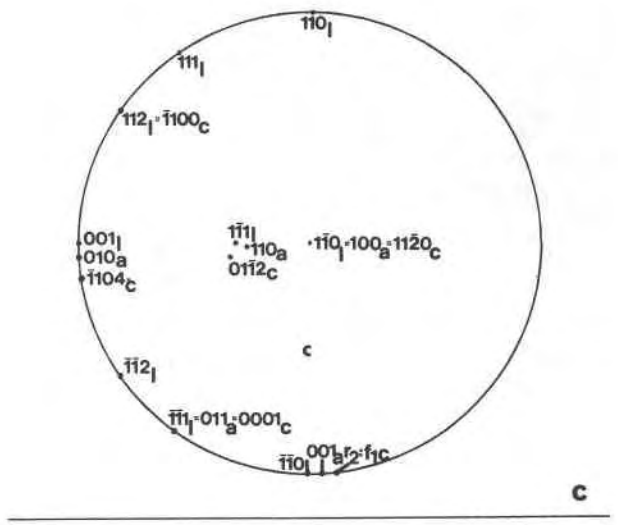


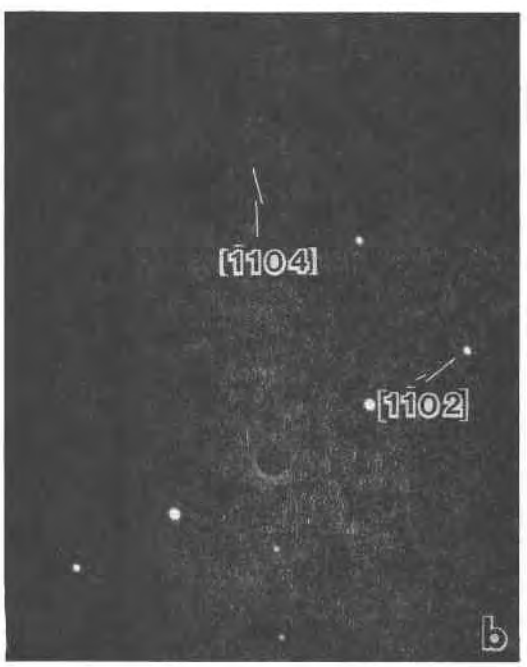


Fig. 6. (a) Selected area diffraction pattern (SAD) of aragonite in a ⟨100⟩ orientation. (b) SAD of post-transformation calcite in a ⟨11$\bar{2}$0⟩ orientation without tilting from (a). (c) Stereographic projection of observed orientation relations.

relationship is recorded between calcite and lime with $(01\bar{1}2)_C \sim (1\bar{1}1)_L$ and $(\bar{1}015)_C \sim (110)_L$ (Fig. 8a, b). If this orientation is then rotated in stereographic projection into a ⟨11$\bar{2}$0⟩ orientation for calcite, the coincident planes are $(11\bar{2}0)_C = (1\bar{1}0)_L$, $(\bar{1}104)_C \sim (001)_L$, and $(0001)_C = (\bar{1}\bar{1}1)_L$ (Fig. 8c).

## Discussion

Observation of the dry-state aragonite–calcite transformation in the TEM reveals topotaxy among low-index crystallographic planes and directions. The coincidence of $(100)_A$ with $(11\bar{2}0)_C$ and $(010)_A$ with $(\bar{1}104)_C$ are predicted based on structural similarities (Fig. 1). This is consistent with the observations of Brown et al. (1962) on metamorphic aragonite. Dasgupta (1964), however, documents the coincidence of $[001]_A$ with $[0001]_C$, $[100]_A$ with $[10\bar{1}0]_C$, and $[110]_A$ with $[01\bar{1}0]_C$ in an X-ray diffraction experiment using aragonite single crystals. Frisia-Bruni and Wenk (1984) note the coincidence of $(010)_A$ with $(11\bar{2}0)_C$ in sedimentary carbonates where replacement occurred through dissolution–reprecipitation. Hiragi et al. (1966) report $(001)_A = (0001)_C$, $(100)_A = (1\bar{2}10)_C$, and $(010)_A = (10\bar{1}4)_C$.

The discrepancies between observed orientation relationships are difficult to rationalize on a purely crystallographic basis. Physical conditions governing nucleation and growth, such as temperature, pressure, and the presence or absence and composition of a fluid phase, may dictate that different kinetic mechanisms may operate which may favor different orientation relations. In the dry-state heating of an aragonite single crystal, for example, a calcite nucleus may grow through coordinated atomic jumps across a high energy interface. In such a transformation the minimum jump distance, hence the minimum strain energy, will occur



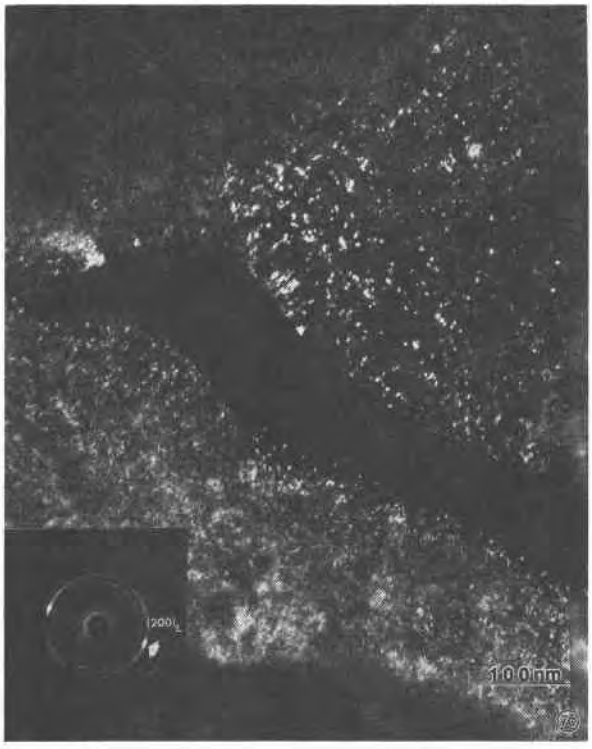


Fig. 7. (a) Darkfield photomicrograph of aragonite plus calcite. Objective aperture is centered on the aragonite (011) reflection. Aragonite appears bright, calcite dark. Note lime rings begin to appear in the SAD and scattered spots in the image signal the onset of decomposition within calcite. (b) Lime rings coarsen and aragonite reflections disappear in the SAD. Lime spots increase in the image. (c) Calcite reflections disappear in the SAD and transformation to lime is ubiquitous in the image. Note widening of the fracture.

between planes and directions in which the two phases are most structurally similar. In this case, orientation relationships are predictable. In the presence of a fluid phase, however, a complicated mechanism involving dissolution, hydration, diffusion, adsorption, and growth, each with its own characteristic rate, is more appropriate.

In this case, orientation relations may depend more on the original orientation and surface perfection of the aragonite substrate and the relative growth rates in crystallographic directions in calcite controlled by diffusion through the fluid phase.

Consistent topotactic relationships observed in the dry-state aragonite–calcite transformation suggest that the mechanism involves minor atomic displacements between the structures rather than long-range diffusion. A coincidence of both $(100)_A = (1\bar{2}10)_C$ and $(001)_A = (0001)_C$, as reported by Hiragi et al. (1966) is unlikely. Although the calcium sublattice appears to be similar between the structures, carbonate groups are displaced by both a **c** trans-

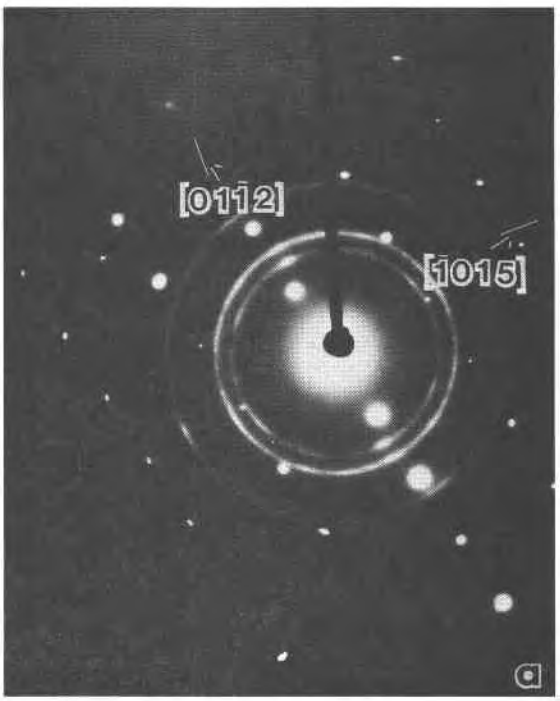


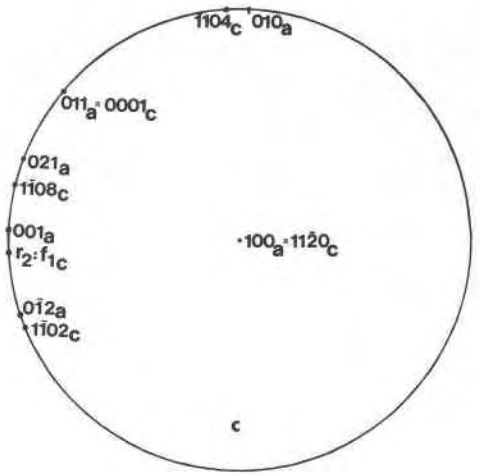


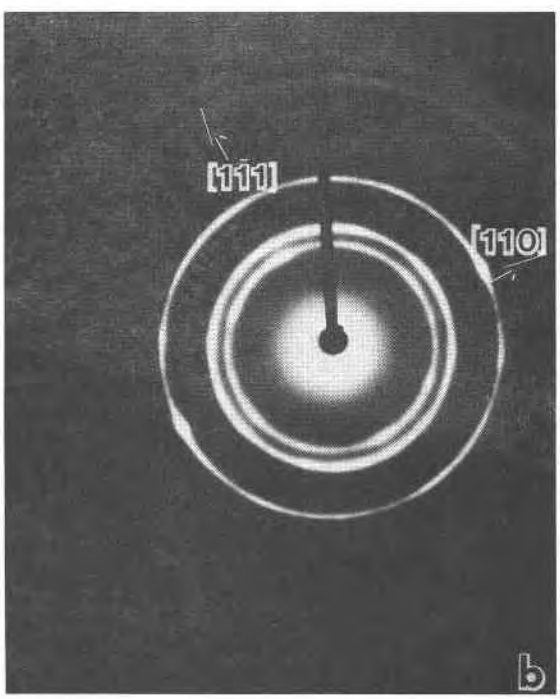


Fig. 8. (a) SAD of calcite in a $\langle 5\bar{2}\bar{3}1\rangle$ orientation with lime rings developing. (b) Pervasive decomposition. Heterogeneous intensity distribution in the rings can be indexed as a single crystal pattern with $[01\bar{1}2]_C \sim [1\bar{1}\bar{1}]_L$ and $[\bar{1}015]_C \sim [110]_L$. (c) Stereographic projection of orientation relations among aragonite, calcite, and lime. Calcite-lime orientation relationship obtained by rotating a calcite $\langle 5\bar{2}\bar{3}1\rangle$ into a $\langle 11\bar{2}0\rangle$, with equal angular rotations for lime, yielding a $\langle 1\bar{1}0\rangle$ lime orientation.

lation (~1.75Å) and a thirty degree rotation in the basal plane (Fig. 9a, b, d, e). Structural sections constructed in the observed orientations from SAD patterns and stereographic projections reveal a closer correspondence of both calcium and carbonate substructures. Smaller rotations and translations of carbonate groups appear necessary in these projections. Although a martensitic transformation is a likely candidate for such a crystallographically controlled transition, the evidence suggests nucleation and growth. Partial dislocations, stacking faults, and plate-shaped precipitates are not observed at or near the aragonite–calcite interface in orientations both parallel and perpendicular to the basal plane. Nucleation is observed at the intersection of planar defects and at the edge of the thin foil. Transformation appears to be controlled by quasi-planar surfaces between individual structural modulations and lamellar twin boundaries.

The observed transformation mechanism may depend on the presence of planar defects in the aragonite precursor. A martensitic transformation, with different orientation relationships, may be possible in more structurally homogeneous samples, in which the density of possible nucleation sites is low. The characterization of microstructures in phases both prior to and following transformation is a critical step in eliciting the transformation mechanism.

The origin of the modulated microstructure is not known. Ordering of solute species, such as $Mg^{++}$, within the aragonite structure is possible, creating domains with slightly different structures. Streaking does not appear in the SAD patterns, however. EDX microanalysis has not

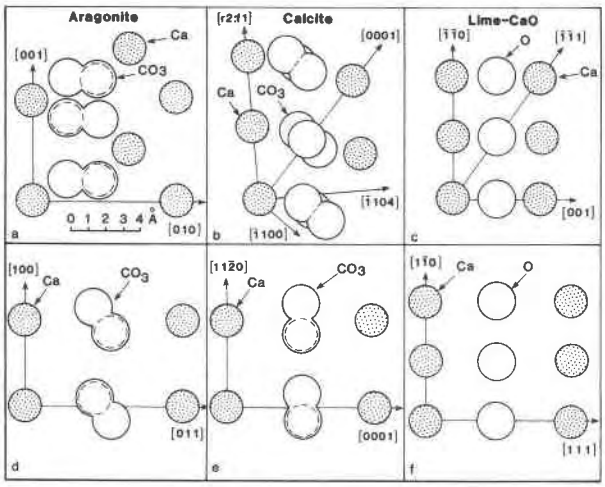


Fig. 9. Structural Projections. (a) Aragonite in a ⟨100⟩ orientation. (b) Calcite in a ⟨1120⟩ orientation with [0001] parallel to [001] in aragonite. (c) Lime in a ⟨110⟩ orientation with $[\bar{1}\bar{1}1]$ parallel to [0001] in calcite. (d) Aragonite in a $\langle 0\bar{1}1\rangle$ orientation. (e) Calcite in a $\langle 1\bar{1}00\rangle$ orientation. (f) Lime in a $\langle \bar{1}\bar{1}2\rangle$ orientation.

been carried out on these domains, although this could help to determine the nature of the modulations.

The decomposition reaction calcite-to-lime plus $CO_2$ exhibits preferred orientation with respect to calcite, as evidenced by SAD patterns and darkfield images. The transformation mechanism may be the driving off of $CO_2$ from the carbonate groups while preserving the general integrity of the and anion arrangement (Fig. 9b, c, e, f). Heterogeneous nucleation and growth of lime may reflect the synchronous decomposition of calcite as it nucleates from aragonite at temperatures above 500°C. The relative reaction rates of aragonite-to-calcite, decomposition of aragonite, and decomposition of calcite have not been determined here, but at 500°C all three reactions appear to proceed synchronously, as evidenced by lime rings in SAD patterns for both aragonite and calcite during aragonite–calcite transformation. Given longer heating time at lower temperatures, these relationships may become more clear, although radiation damage becomes more significant with increased exposure time.

## Conclusions

On a microstructural scale this study supports the mechanism proposed by Carlson and Rosenfeld (1981) and Carlson (1982, 1983) of heterogeneous topotactic nucleation and growth for the dry-state aragonite–calcite transformation. An orientation relationship in which $(100)_A = (11\bar{2}0)_C$, $(010)_A \sim (\bar{1}104)_C$, and $[001]_A \sim [r_2 : f_1]_C$ is consistently observed, in agreement with Brown et al. (1962). The decomposition reaction may be the driving off of $CO_2$ molecules from a relatively rigid cation framework, collapsing the structure slightly and creating porosity but preserving an orientation relationship in which $(1\bar{1}0)_L = (11\bar{2}0)_C$, $(\bar{1}\bar{1}1)_L \sim (0001)_C$, and $(001)_L \sim (\bar{1}104)_C$.

## Acknowledgments

The authors wish to thank Ken Westmacott and Dave Ackland at the National Center for Electron Microscopy at the Lawrence Berkeley Laboratory for the opportunity to use the instrument and continued support for this research. This study was funded through NSF grants EAR 78-23848, 83-05865, and ACS grant PRF 13615-AC2.

## References

Barrett, C. and Massalski, T. B. (1980) Structure of Metals. Pergamon, Oxford.

Brown, W. H., Fyfe, W. S., and Turner, F. J. (1962) Aragonite in California glaucophane schists, and the kinetics of the aragonite–calcite transformation. Journal of Petrology, 3, 566–582.

Burrage, B. J. and Pitkethly, D. R. (1969) Aragonite transformations observed in the electron microscope. Physica Status Solidi, 32, 399–405.

Carlson, W. D. (1982) Aragonite–calcite nucleation kinetics; an application and extension of Avrami transformation theory. Journal of Geology, 91, 57–71.

Carlson, W. D. (1983) The polymorphs of $CaCO_3$ and the aragonite–calcite transformation. In R. J. Reeder, Ed., Carbonates: Mineralogy and Chemistry MSA Reviews in Mineralogy, v. 11, 191–225.

Carlson, W. D. and Rosenfeld, J. L. (1981) Optical determination of topotactic aragonite–calcite growth kinetics: metamorphic implications. Journal of Geology, 89, 615–638.

Dasgupta, D. R. (1964) The oriented transformation of aragonite into calcite. Mineralogical Magazine, 33, 924–928.

Frisia-Bruni, S. and Wenk, H.-R. (1984) Replacement of aragonite by calcite in sediments from the San Cassiano Formation (Italy). Journal of Sedimentary Petrology (in press).

Gillet, P. and Madon, M. (1982) Un modele de dislocations pour la transition aragonite–calcite. Bulletin Mineralogique, 105, 590–597.

Hiragi, Y., Kachi, S., Tagada, G., and Nakanishi, N. (1966) Title unavailable. Nippon Kagaka Zarshi, 87, 1308–1311.

Madon, M. and Gillet, P. (1984) A theoretical approach to the calcite–aragonite transition: application to laboratory experiments. Earth and Planetary Science Letters, 67, 400–414.

Van Tendeloo, G., Van Landuyt, J., and Amelinckx, S. (1975) Electron microscopic observations of the domain structure and the diffuse electron scattering in quartz and in aluminum phosphate in the vicinity of the alpha–beta transition. Physica Status Solidi, (A)30, K11–15.

Wenk, H.-R., and McTigue, J. W., Jr. (1983) Aragonite–calcite and calcite–lime transformations observed in situ in the high voltage transmission electron microscope. In Proceedings of the Seventh International Conference on High Voltage Electron Microscopy, Berkeley, California, 347–352.

*Manuscript received, January 10, 1985;*
*accepted for publication, July 25, 1985.*